Building Alloys from Single Atoms: Au−Pd Chains on NiAl(110)†

N. Nilius,‡ T. M. Wallis,§ and W. Ho*

Department of Physics and Astronomy and Department of Chemistry, University of California, Irvine, California 92697-4575

Received: February 26, 2004; In Final Form: April 20, 2004

Well-ordered mono-elemental and alloy chains have been assembled from single Au and Pd atoms on a NiAl(110) surface with a scanning tunneling microscope. Spatially resolved conductance measurements revealed the development of quantum well states in the different atomic chains, which are aligned on free-electron like bands. Effective electron mass and onset energy of states in mixed Au−Pd chains lie between the values obtained for pure Au and Pd chains. The results demonstrate effective hybridization of Au and Pd induced states to a delocalized electronic system, in correspondence with the perfect miscibility of the respective bulk materials.

Metal alloys form a versatile class of materials with novel mechanical, electronic and chemical behavior. The specific properties of alloys can be adjusted over a wide range by changing elemental composition and alloying conditions. For example, the optical absorption band in Ag−Au particles can be continuously shifted from the silver to the gold position by increasing the Au mass ratio in the alloy.[1] The catalytic properties of Pd deposits for the butadiene hydrogenation increase dramatically when Pd is substituted by Ni or Cu atoms.[2] These advantages make alloys indispensable for various, economically important technologies in material science and heterogeneous catalysis.

The alloying of metals has been studied extensively for bulk materials, using nonlocal diffraction and spectroscopy techniques. A more local picture could be obtained on surfaces, where the scanning tunneling microscope (STM) has enabled studies of surface alloys on the atomic scale.[3−5] The alloying process was investigated from a structural point of view, determining the atomic arrangement of the different species as a function of alloying temperature, lattice mismatch, strain accommodation, and surface segregation.[6,7] The influence of alloy formation on electronic properties is not well characterized yet, specifically when the local arrangement of atoms determines the electronic structure of the alloy. In disordered Au−Pd alloys, the interaction of Au and Pd induced electronic states leads to the formation of either delocalized bands or spatially confined states, depending on the local alloy composition.[8] Experiments on single-atom point contacts demonstrated the blocking of the current between two Au leads due to the presence of a single Pd atom in the path.[9] Both results are especially intriguing,[8,9] as Pd and Au are miscible in the whole composition range and show a gradual shift of the alloy properties from the Au to the Pd side of the phase diagram.[10]

The absence of long-range order in many alloys complicates the situation. Except for distinguished points in the phase diagram, atoms of different species randomly occupy the lattice sites in the crystal. Especially in confined systems containing only few tens of atoms, random disorder causes large fluctuations in the electronic properties. Dramatic effects induced by the position change of a single atom in one-dimensional (1D) chains have been predicted by model calculations.[11,12] The interplay between structural and electronic properties on the atomic scale could be examined only for mass-selected alloy particles in cluster beams so far.[13]

This paper demonstrates a different approach, which combines the preparation of well-defined alloy structures on a metal surface and their electronic characterization with an STM. The experiments adapt atom manipulation techniques with the STM tip, introduced earlier to construct Au chains from single atoms on a NiAl(110) surface.[14,15] The assembly of atomic chains induces the development of a quantum well, characterized by a number of discrete energy levels with parabolic dispersion.[16] To investigate the influence of chain composition on the electronic structure, pure Au and Pd as well as Au−Pd alloy chains were constructed on NiAl(110). Gold and palladium were chosen for the alloy formation, as both elements differ in their intrinsic electronic properties. Whereas the *6s* orbital in isolated Au atoms is occupied by a single electron, the corresponding *5s* level in Pd atoms is empty and the highest occupied orbital has *d* character.

The experiments were performed with an ultrahigh vacuum STM operated at 12 K.[17] The NiAl(110) surface was cleaned by cycles of Ne^+ sputtering and annealing to 1300 K. STM topographic images of the surface show the alternation of Al rows and Ni troughs running along the NiAl [001] direction. Equivalent rows are separated by 4.08 Å; atoms along the rows have an interatomic spacing of 2.89 Å. Individual Au and Pd atoms were evaporated from two alumina crucibles and deposited at 12 K onto the surface. At this temperature, atom diffusion is inhibited and single atoms were observed as protrusions in STM topographic images (Figure 1). The apparent height of Au and Pd atoms exhibits a characteristic dependence on the sample bias. Below +1.0 V, Au and Pd monomers are almost equivalent in height (Figure 1A). With increasing voltage, the apparent height of Au atoms quickly increases and clearly exceeds the Pd height in images taken at +2.0 V (Figure 1B). At higher voltages, Au and Pd atoms are imaged with almost

† Part of the special issue "Gerhard Ertl Festschrift".

* Corresponding author. E-mail: wilsonho@uci.edu.

‡ Present address: Fritz-Haber-Institut, Faradayweg 4-6, D-14195 Berlin, Germany.

§ Present address: National Institute of Standards and Technology, Boulder, CO 80305.

10.1021/jp049127r CCC: $27.50
Published on Web 06/08/2004

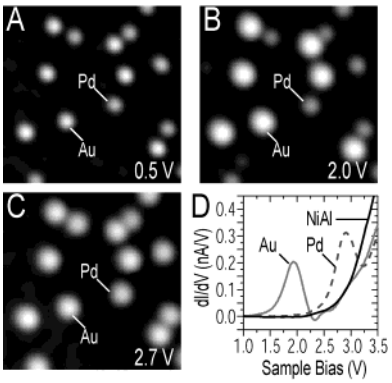

Figure 1. STM topographic images of individual Au and Pd atoms on NiAl(110) taken at (A) 0.5 V, (B) 2.0 V, and (C) 2.7 V ($I = 1.0$ nA). Each image is 60 Å × 60 Å in size. The strong bias dependence of the apparent height is caused by distinct resonances in the LDOS of Au and Pd atoms. (D) dI/dV spectra of single Au and Pd atoms and bare NiAl(110), taken at a tunneling gap set with $U_{sample} = 3.0$ V, $I = 1$ nA. The resonance states induced by single Au and Pd atoms are observed as prominent dI/dV peaks at 1.95 and 2.80 V, respectively.

identical corrugation (Figure 1C). The distinct height difference at +2.0 V sample bias enables an unequivocal differentiation of both species on the NiAl surface.

The origin of the height difference can be understood from differential conductance (dI/dV) measurements as a function of bias voltage, detected with lock-in technique. The dI/dV signal provides a measure of the local density of states (LDOS) of the sample surface. In contrast to the smoothly increasing dI/dV intensity of the NiAl surface, spectra of Au and Pd atoms reveal prominent resonances at 1.95 and 2.80 V, respectively (Figure 1D). The resonances represent unoccupied energy levels induced by the single atoms. For Au_1, the dI/dV peak has been identified by density functional calculations as a hybridization of the Au *6sp* atomic orbital and NiAl electronic states, and is localized in a pseudo gap of NiAl bulk bands.[18] A similar hybridization can be assumed for Pd atoms; however, the absence of a valence electron in Pd ($5s^0$) compared to Au ($6s^1$) shifts the resonance to higher energies. The presence of distinct peaks in dI/dV spectroscopy provides an additional way to distinguish between Pd and Au atoms on the surface.

Deposited metal atoms could be manipulated on NiAl(110) at small tip−sample distances, adjustable via the tunneling resistance V/I. The onset for the manipulation of Au atoms was determined to be 150 kΩ. Pd manipulation required a resistance of 50 kΩ, indicating a stronger Pd interaction with the substrate. Despite these differences in the manipulation regime, individual Au and Pd atoms could be assembled into pure and mixed chains using the Ni troughs as natural template (Figure 2). The characteristic height difference between Au and Pd monomers disappears in alloy chains, which are imaged with uniform height independent of the applied sample bias. The disappearance of the height signature indicates strong coupling between Au and Pd electronic states.

Figure 2A shows the development of the electronic structure in Au−Pd alloy chains as a function of chain length. For the Au−Pd dimer, the initial single-atom resonances remain visible, however, with red-shifted peak positions due to the presence of the neighboring atom (Au: 1.95 → 1.70 V; Pd: 2.80 → 2.75 V). The formation of a Au−Pd−Au trimer creates a new electronic state at 1.30 V, which is delocalized over the aggregate. Adding alternately Au and Pd atoms to the chain leads to a continuous red-shift of the low-energy dI/dV peak, which converges to 1.05 V for a $Au(PdAu)_5$ alloy chain (Figure

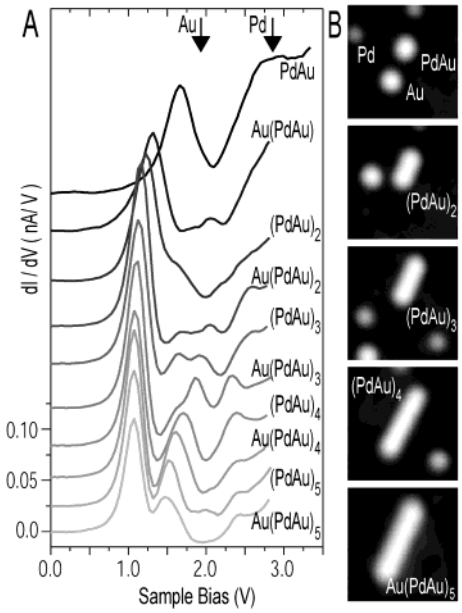

Figure 2. (A) dI/dV spectra taken over the center of Au−Pd alloy chains with increasing length. The tunneling gap was set with $U_{sample} = 3.0$ V, $I = 1$ nA. The positions of the Au_1 and Pd_1 resonance states are marked by arrows. The coupling of these orbitals leads to the formation of quantum well states in the Au−Pd alloy chains, whereby the lowest energy state dominates the density of states in the spectra. (B) STM topographic images of selected Au−Pd alloy structures on NiAl(110) ($U_{sample} = 2.0$ V, $I = 1$ nA). The size of each image is 40 Å × 40 Å.

2A). Additional resonances appear at higher energies and move toward the Fermi level with increasing chain length. The development of the electronic structure in Au−Pd alloy chains qualitatively follows the trend observed for pure Au and Pd chains.[14,19]

Further information on the electronic properties of Au_{11}, Pd_{11}, and $Au(PdAu)_5$ chains can be deduced from spatially resolved conductance measurements taken along the chain axis. For all three chains, the low-energy dI/dV peak dominates spectra taken over the chain center. Its energy position shifts from 0.75 eV for Au_{11}, to 1.05 eV for $Au(PdAu)_5$ and 1.50 eV for Pd_{11} chains. The dI/dV signal at higher sample bias shows characteristic intensity modulations along the chain axis. The intensity oscillations are obvious in cross sections through the spectral series at a constant bias. Each curve in Figure 4A reflects the dI/dV intensity variations in the alloy chain for a fixed bias voltage between 0.87 and 2.89 V. For specific bias values (thick lines), pronounced oscillations with one to five maxima are visible along the chain. At first glance, these intensity modulations resemble standing-wave patterns of 1D quantum well states, characterized by $n - 1$ nodes for the nth energy level. Spatially resolved dI/dV oscillations of the pure Au and Pd chains can be found elsewhere.[14,20]

Similar conductance patterns were derived from dI/dV micropscopic images, mapping the dI/dV signal at constant bias above the atomic chains. In correspondence to spectroscopic measurements, a number of maxima and minima were detected along the chain axis, which increases with the applied sample bias (Figure 4B). Figure 5 compares the dI/dV maps for Au_{11}, $Au(PdAu)_5$, and Pd_{11} chains on NiAl(110). Similar intensity patterns were observed in all three cases, however, at bias positions shifted in accordance to the dI/dV peaks. Images in the first row result from a superposition of the first and second quantum well state. The following two rows of images show the second and third state, characterized by one and two nodes

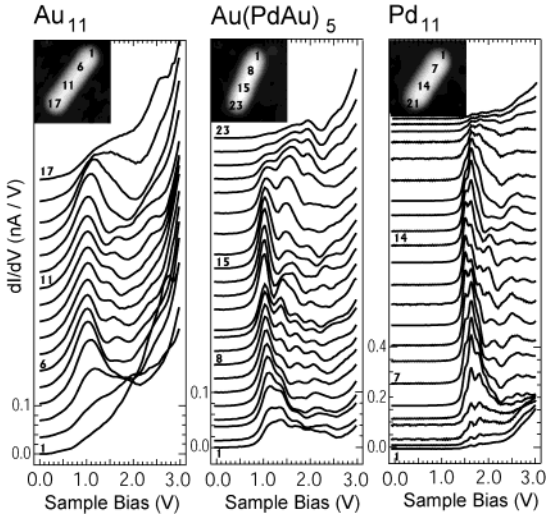

Figure 3. dI/dV spectra taken in equidistant steps along the axis of a Au_{11}, $Au(PdAu)_5$, and Pd_{11} on NiAl(110). The tunneling gap was set with $U_{sample} = 3.0$ V, $I = 1$ nA. Tip positions for spectroscopy are shown in the insets. The spectra result from the overlap of several quantum well states in the respective chains.

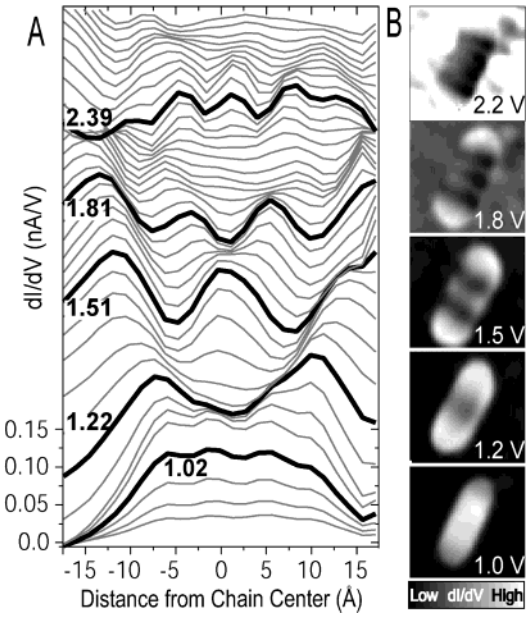

Figure 4. (A) dI/dV intensity patterns at constant bias along the axis of a $Au(PdAu)_5$ chain. Each curve represents a cross section through the spectral series shown in the center panel of Figure 3. The dI/dV oscillations reflect the interference of standing wave patterns of electronic states with different wavenumbers in the chain. Thick solid lines mark the energy of distinct quantum well states in $Au(PdAu)_5$. (B) dI/dV microscopic images of a $Au(PdAu)_5$ chain on NiAl(110) taken at the energy position of the first five quantum well states ($I = 1.0$ nA). Each image is 40 Å × 40 Å in size.

along the chain. The fourth state is located between the bias values selected for the fourth and fifth rows. Finally, the sixth row of images depicts standing wave patterns associated with the fifth quantum well state in the chains. The alternation of maxima and minima is clearest for dI/dV maps of Pd chains, which indicates larger energy separation and smaller intrinsic width of the respective quantum well states.

The energy position of quantum well states in atomic chains was determined by fitting the experimental dI/dV oscillations to the squared wave functions of a "particle-in-a-box" model with infinite walls.[14,16] To account for the finite depth of the

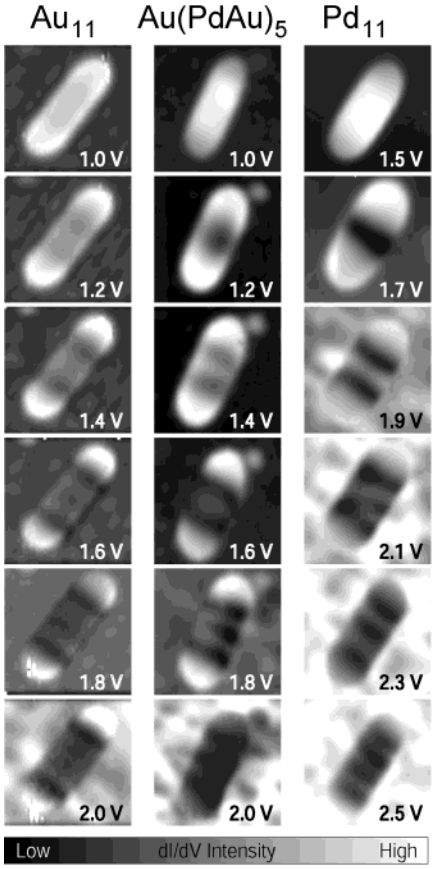

Figure 5. dI/dV microscopic images of Au_{11}, $Au(PdAu)_5$, and Pd_{11} on NiAl(110) taken at the indicated sample voltages ($I = 1$ nA). Each image has a size of 40 Å × 40 Å. The images show standing wave patterns of quantum well states with different wavenumbers in the respective chains.

potential, the length L of the well was treated as an adjustable parameter. Wave functions in an idealized quantum well are sinusoids with wavenumber $k_n = n\pi/L$, characterized by $n - 1$ nodes for the nth eigenfunction. As more than one wave function contributes to the dI/dV signal, a sum of squared sinusoids was used in the fitting procedure. A bias-dependent prefactor c_n accounts for the spectral weight of individual wave functions in the experimental spectra: $dI/dV\,(V) \propto \Sigma_n\, c_n(V)\,[\sin(k_n x)]^2$. The procedure yields a Gaussian dependence on V for each coefficient, whereby the maximum in c_n is taken as the energy position of the nth quantum well state. The interrelation between level energies and associated wavenumber follows the dispersion of electronic states in an idealized quantum well: $E_n(k) = E_0 + (\hbar^2/2m_{eff})\,k_n^2$. For all three chains, the (E_n, k_n^2) pairs show the expected linear proportionality with a slope corresponding to the effective electron mass of the quantum well states (Figure 6A). Effective masses m_{eff} were determined to $0.50m_e$ for Au_{11}, $0.56m_e$ for $Au(PdAu)_5$, and $0.65m_e$ for Pd_{11}. Figure 6B shows the evolution of the low-energy dI/dV resonance with an increasing number of atoms in the three chains. The size-dependent shift levels out for more than 10 atoms assembled in the chain and reflects the expected L^{-2} dependence on the chain length L. The onsets of quantum well states E_0 were determined to 0.75 V for Au_{11}, 1.05 V for $Au(PdAu)_5$, and 1.5 V for Pd_{11} chains. Figure 6C shows the experimental LDOS for the three chains, derived from averaging dI/dV spectra along the chain axis and subtracting a NiAl background signal. In addition to the blue-shift in onset energy E_0, a narrowing of the dI/dV resonances is observed for an increasing Pd content in the chains.

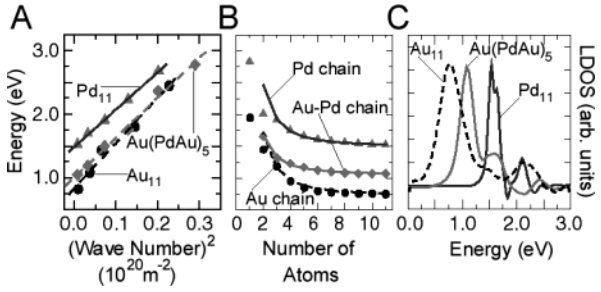

Figure 6. (A) Energy position as a function of squared wavenumber for quantum well states in Au_{11}, $Au(PdAu)_5$, and Pd_{11} chains on NiAl-(110). The level energies were determined by fitting dI/dV intensity patterns along the chains to a 1D "particle-in-a-box" model. The straight lines represent best fits to the data. The slope is proportional to the effective electron mass of the quantum well states. (B) Dependence of the position of the low-energy dI/dV peak on the number of atoms in Au, Au−Pd, and Pd chains. Au and Pd atoms have been alternately added to the alloy chain [AuPd, AuPdAu, $(AuPd)_2$, $(AuPd)_2Au$, $(AuPd)_3$...]. The lines represent best L^{-2} fits as a function of chain length L. (C) Experimental LDOS for Au_{11}, $Au(PdAu)_5$, and Pd_{11}, obtained from averaging dI/dV spectra along the chain and subtracting a NiAl background signal.

The assembly of pure and mixed atomic chains on NiAl-(110) initiates the development of quantum well states with parabolic dispersion. Onset energy and effective mass of the states in $Au(PdAu)_5$ alloy chains fit between those values for pure Au_{11} and Pd_{11} chains. The presence of delocalized electronic states demonstrates effective hybridization of Au and Pd induced orbitals, despite an energy difference of 0.85 eV between the single-atom resonances. The increase in effective electron mass from the Au chain to the Au−Pd and the Pd chain indicates a decreasing overlap between neighboring orbitals in the chains. This interpretation is consistent with a larger spatial extension of the initial Au *6sp* orbital compared to the Pd *5sp* level. The energy difference between the Au_1 and Pd_1 resonance states does not determine the hybridization efficiency, because otherwise the effective mass should be largest in the Au−Pd alloy and not in the pure Pd chains. The dominance of Au orbitals for the Au−Pd hybridization is reflected in the electronic properties of alloy chains, which are closer to the behavior of Au_{11} than of Pd_{11}. The decreasing orbital overlap in mixed and pure Pd chains also leads to quantum well states with smaller intrinsic width. The Pd_{11} chain shows consequently the narrowest dI/dV resonances (Figure 3) and the clearest standing-wave patterns in the experiment (Figure 5), followed by the alloy chain. The electronic properties of Au−Pd chains do not switch abruptly between aggregates containing a surplus Au versus Pd atom. In fact, the electronic signature develops gradually when Au and Pd atoms are alternately added to the alloy chain, which is manifested by a continuous downshift of the low-energy dI/dV peak with increasing chain length (Figure 6 B). The electronic properties of regular Au−Pd chains are obviously dominated by the number of interacting orbitals and not so much by their chemical identity.

The observed mixing of Au and Pd induced electronic levels in 1D alloy chains is inline with the perfect miscibility of Au and Pd in the bulk phase.[10] The formation of delocalized quantum well states, however, depends on the local order in the alloy structure. A grouping of Au and Pd atoms may cause a completely different electronic behavior than observed in regular Au−Pd alloy chains. A spatial separation of Au and Pd atoms in the chain could even result in a disintegration of the quantum well into a Au and a Pd section. The role of disorder and impurities in Au−Pd alloy structures will be the topic of a forthcoming paper.[19]

In conclusion, the influence of elemental composition on 1D electronic systems was investigated by assembling single Au and Pd atoms to mono-elemental and alloy chains on a NiAl-(110) surface. Standing-wave patterns have been observed in Au_{11}, $Au(PdAu)_5$, and Pd_{11} chains, manifesting the development of quantum well states. The dispersion of electronic states in the $Au(PdAu)_5$ chain lies between the values obtained for pure Au_{11} and Pd_{11} chains, indicating effective coupling between Au and Pd orbitals. As the sequence of atoms along the chain axis can be controlled, the role of impurities and disorder can be examined and an electronic and chemical characterization of bimetallic systems becomes possible on the atomic level.

Acknowledgment. This material is based on work supported by the National Science Foundation under Grant No. 0102887. N.N. gratefully acknowledges the Deutsche Forschungsgemeinschaft for support.

References and Notes

(1) Link, S.; Wang, Z. L.; El-Sayed, M. A. *Phys. Chem. B* **1999**, *103*, 3529.
(2) Hermann, P.; Guigner, J. M.; Tardy, B.; Jugnet, Y.; Simon, D.; Bertolini, J.-C. *J. Catal.* **1996**, *163*, 169; Constant, L.; Ruiz, P.; Abel, M.; Rohbach, Y.; Porte, L.; Bertolini, J. C. *J. Catal.* **2001**, *14*, 1.
(3) Bach Aaen, A.; Laegsgaard, E.; Ruban, A. V.; Stensgaard, I. *Surf. Sci.* **1998**, *408*, 43.
(4) Heinze, S.; Abt, R.; Buegel, S.; Gilarowski, G.; Niehus, H. *Phys. Rev. Lett.* **1999**, *83*, 4808.
(5) Wouda, P. T.; Schmid, M.; Nieuwenhuys, B. E.; Varga, P. *Surf. Sci.* **1998**, *417*, 292.
(6) Koel, B. E.; Sellidj, A.; Paffett, M. T. *Phys. Rev. B* **1992**, *46*, 7846.
(7) Robach, Y.; Abel, M.; Porte, L. *Surf. Sci.* **2003**, *526*, 248.
(8) Nahm, T. U.; Jung, R.; Kim, J. Y.; Park, W. G.; Oh, S. J.; Park, J. H.; Allen, J. W.; Chung, S. M.; Lee, Y. S.; Whang, C. N. *Phys. Rev. B* **1998**, *58*, 9817.
(9) Enomoto, A.; Kurokawa, S.; Sakai, A. *Phys. Rev. B* **2002**, *65*, 125410.
(10) Meyer, R. J. *Gmelin Platin Part A*; Verlag Chemie: Weinheim, 1951; p 691.
(11) Lang, N. D. *Phys. Rev. B* **1995**, *52*, 5335.
(12) Gonzalez, R. R.; Schulz, P. A. *Phys. Rev. B* **1998**, *57*, 14766.
(13) Koyasu, K.; Mitsiu, M.; Nakajima, A.; Kaya, K. *Chem. Phys. Lett.* **2002**, *358*, 224.
(14) Nilius, N.; Wallis, T. M.; Ho, W. *Science* **2002**, *297*, 1853.
(15) Wallis, T. M.; Nilius, N.; Ho, W. *Phys. Rev. Lett.* **2002**, *89*, 236802.
(16) Mills, G.; Wang, B.; Ho, W.; Metiu, H. *J. Chem. Phys.* **2004**, *120*, 7738.
(17) Stipe, B. C.; Rezaei, M. A.; Ho, W. *Rev. Sci. Instrum.* **1999**, *70*, 137.
(18) Nilius, N.; Wallis, T. M.; Persson, M.; Ho, W. *Phys. Rev. Lett.* **2003**, *90*, 196103.
(19) Wallis, T. M.; Nilius, N.; Ho, W. In preparation.
(20) Nilius, N.; Wallis, T. M.; Ho, W. In preparation.